Journal of Renewable Materials

Tech Science Press

Preparation and Properties of Guiqi Polysaccharides/Chitosan/Alginate Composite Hydrogel Microspheres

Xiaoliang Zhao[1,#], Yuting Wang[1,#], Xiuying Pu[1], Jianzhong Ma[1], Feifan Leng[1], Yonggang Wang[1], Yanling Wang[1], Shuhong Yang[1], Fen Ran[2] and Weijie Zhang[1,*]

[1]School of Life Science and Engineering, Lanzhou University of Technology, Lanzhou, 730050, China.

[2]School of Material Science and Engineering, Lanzhou University of Technology, Lanzhou, 730050, China.

[#]These authors have an equal contribution to the work and should be considered as the co-first author.

[*]Corresponding Author: Weijie Zhang. Email: twz1514@126.com.

Abstract: A series of the Guiqi polysaccharides/chitosan/alginate composite hydrogel microspheres (GPcM) with different particle sizes were prepared with Guiqi polysaccharides (GP), chitosan (CS) and sodium alginate (Alg). The optimum preparation process was also determined by single factor and orthogonal experiment analysis. The GPcM were characterized by fourier transform infrared spectroscopy (FT-IR), scanning electron microscope (SEM), drug loading efficiency test (LE), encapsulation efficiency test (EE) and *in vitro* release study. The results showed that the Guiqi polysaccharides chitosan hydrogel (GPCH) and sodium alginate hydrogel (SAH) formed a crossover system in GPcM. The GPcM have a uniform particle size ranging from 395.1μm to 841.5μm. The drug loading efficiency and encapsulation efficiency of the GPcM were 56.3% and 72.6%, respectively. The bovine serum albumin (BSA) loaded in the GPcM released slowly within 180 h. The results suggested that the GPcM may have potential application value in drug sustained and controlled release system.

Keywords: Guiqi polysaccharides; composite hydrogel microspheres; cross-linker; drug loading

1 Introduction

Microspheres fabricated from biodegradable polymers have been widely used in the research of tissue engineering for their excellent biocompatibility, degradability and large surface area. Acting as microcarriers or scaffolds, microspheres can promote cells proliferation and repair of tissue defect [1-3]. Polysaccharides, as a kind of cheap and easily accessible biopolymers, have been widely studied in water-soluble model drugs loading microsphere matrix. Chitosan (CS), starch, and sodium alginate (Alg) derived microspheres show perfect prosperity in controlled release drug delivery [4-9]. However, the above-mentioned polysaccharides materials are generally inert. They are not satisfactory in biological effect and drug loading. If the microsphere matrix has the certain effect which can bring synergistic effects, the required drug loading will decrease. A kind of composite microsphere matrix would be promising solutions.

Some traditional medicine, like *Angelica sinensis* and *Astragalus membranaceus* (Fisch.) Bunge, are multifunctional and popularly used in China for more than 2,000 years [10]. Recent studies showed Guiqi polysaccharides (GP) *extracted from compound of A. sinensis* and *A. membranaceus* showed good biological activity [11], such as neuroprotection [12], antioxidation [13], antiinflammatory [14], antiviral [15], antitumor [16], antiaging [17] and immunomodulatory activities [18], and so on. So GP is the right choice for improvement of the biological effects of composite hydrogel microspheres.

CS is a unique polymer for tissue scaffolds, especially for hydrogels for its innocuity and antibacterial effect [19]. Alg is another polymer usually used for hydrogel preparation. Its abundant oxygen-containing functional groups such as carboxyl groups and hydroxyl groups, can combined with some divalent cations such as Ca^{2+}, Ba^{2+}, Zn^{2+}, and form a three-dimensional network structure hydrogel with good hydrophobicity. Alg can be used as a template for preparing a composite hydrogen [20,21]. While, as we know, though they can form hydrogel easily, CS and Alg have not so much biological effect to produce synergistic effect with primary drugs they loaded. An effective method to meet the requirement is that prepare composite materials with CS, Alg and GP by cross-linking.

Electrostatic spraying (ES) is a potential technique for hydrogel microsphere preparation. When coming out of the ES nozzle, the input material is charged and broken down into smaller and relatively monodisperse particles/droplets, then deposited on the trajectory due to electrostatic attraction [22]. ES has attracted widespread attention in food industry due to its material savings and high efficiency [23]. When the entering material is liquid, ES can control particle size and increase particle coverage simultaneously [24] and improve overall coating quality [23]. The efficiency of the ES is not only affected by the spray parameters, but also by the nature of the material [25]. At present, ES is mostly used for spraying the surface of materials, and is less used for preparing microspheres for drug delivery. In this experiment, ES, as a novel process, was used to prepare bioactive composite microspheres.

To meet the above mentioned requirement, in this study, Guiqi polysaccharides/chitosan/alginate composite hydrogel microspheres (GPcM) were prepared by electrostatic sprayin. The chemical and physical properties of microspheres such as morphology, particle size, drug loading, encapsulation efficiency and *in vitro* release was evaluated at the same time.

2 Materials and Methods

2.1 Materials

Chitosan (CS) (exacted from crab shells; Mw, 235 kDa, deacetylation degree, 93.7%) was purchased from Jinhu Crust Product Co., Ltd. (Qingdao, China). *Angelica sinensis* and *Astragalus membranaceus* (Fisch.) Bunge was bought from Yellow River Medicinal Materials Market (Lanzhou, China). Chloroacetic acid and sodium periodate ($NaIO_4$) were purchased from Tianjin Evergreen Chemical Reagent Manufacturing Co., Ltd. (China). Coomassie brilliant blue (CBB) and BSA supplied by Biotopped (China). All other chemicals used were analytical grade, without further purification. Ultrapure water (Milli-Q Gradient A10 Water Purification System, Millipore Corporation, MA, US), it was used to prepare all solutions.

2.2 Preparations of Composite Hydrogel Microspheres

2.2.1 Extraction of GP

The GP was extracted from *A. sinensis* and *A. membranaceus (*Fisch.) Bunge according to the method of the literature [26,27]. *A. sinensis* and *A. membranaceus* (Fisch.) Bunge (*w*/*w* 1:5) was pulverized, degreased with 5 volumes ethanol at 80°C for 2 times (2 h each time), and extracted with 20 volumes of distilled water at 80°C for 3 times (3 h each time). After then, the extracting solution was centrifuged and filtrated, and then precipitated with four volumes of 95% ethanol. The precipitate was dissolved in distilled water and dialyzed for 72 h, and then lyophilized to obtain GP.

2.2.2 Oxidation of GP

Oxidized GP (oGP) was prepared by oxidation with sodium periodate [28]. In brief, 3 g GP were dissolved in 120 mL ethanol/water (1:1 *v*/*v*) and stirred for 2 h, then 1.42 g of sodium periodate was added to the reaction system and stirred for 8 h in dark environment. After that, 0.4 mL ethylene glycol was added to the reaction system and stirred for 1 h. Finally, the reaction solution was precipitated with 5

volumes of 95% ethanol to obtain oGP. Determination of aldehyde group concentration in oGP by hydroxylamine hydrochloride method [29].

2.2.3 Synthesis and Characterization of CMC

Using chitosan (CS) as raw material, carboxymethyl chitosan (CMC) with good water solubility was prepared by electrophilic substitution reaction [28]. Respectively, CS (5 g) was added into 25 mL of NaOH (40%, *w*/*w*) solution at -20°C overnight. Then chloroacetic acid solution (20 g dissolved into 100 mL of isopropanol) was added into the frozen chitosan suspension dropwise for 30 min. After that, the mixture was continuously stirred at 20°C for 2 h, and the same stirred at 60°C for 2 h. Finally, the resultant was filtered and washed three times with 95% ethanol. After drying by oven at 40°C, the final product of CMC was obtained [29]. Determination of the degree of substitution of *N*, *O*-carboxymethyl chitosan by titration [30].

2.2.4 Preparation of GPCH

Prepared the Guiqi polysaccharides/chitosan hydrogel (GPCH) with oGP and CMC as substrates. In brief, oGP and CMC were dissolved into 10 mL distilled water to form 5 and 10% (w/w) solutions, respectively. According to the volume ratio of 1:1, oGP and CMC solutions were mixed at room temperature with gentle stirring, then the mixed solutions were placed at 25°C for 10 min to form the hydrogels (GPCH).

2.2.5 Preparation of GPAH

0.5 g of Alg was added to 10 mL of distilled water to prepare a 5% Alg solution. 2 mL of 2% $CaCl_2$ solution was added dropwise to the Alg solution, 4 mg of GP was dissolved in 2 mL of distilled water to prepare a 2 mg/mL polysaccharide solution, and the mixture was allowed to stand for 20 min to obtain sodium alginate hydrogel (GPAH).

2.2.6 Preparation of GPcM

In industry, chitosan microspheres were usually prepared by the method of spray drying [31]. The particle size of the microspheres depends on the spray speed, spray temperature and degree of crosslinking [32]. Firstly, 100 mg oGP was dispersed in 10 mL deionized water, and 100 mg CMC was dispersed in 20 mL deionized water. After that, oGP solution and CMC were mixed together, then 4% Alg solution was added into the mixed solution. The GPcM were obtained immediately by dropping the uniform GP-Alg mixed solution into $CaCl_2$ solution (2 wt%) in ES at the speed of 10 mL/min (Scheme 1).

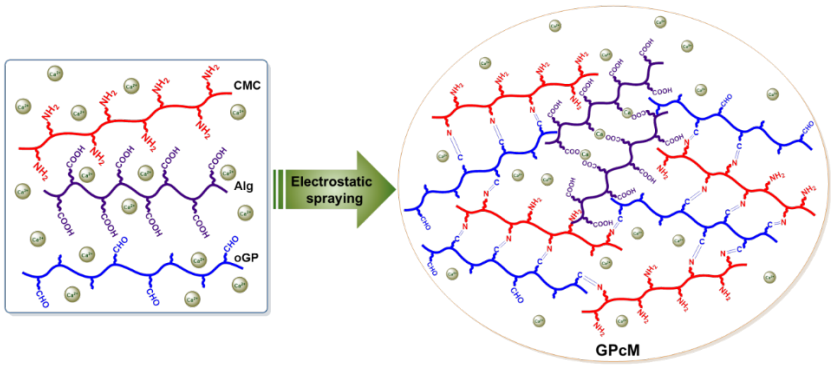

Scheme 1: Schematic diagram of preparation principle of GPcM by ES

2.2.7 Preparation Process Optimization of GPcM

When the GPcM were prepared by ES, the preparation conditions had a significant effect on the particle size of the microspheres. Hydrogel microspheres were prepared at different voltages from 10 kV to 16 kV and microsphere size was measured microscopically through a hemocytometer. In addition, the matrix concentration of the GPcM also has an effect on the particle size. GPcM were prepared with different concentrations of material under optimal voltage conditions. The concentration gradient is as Tab. 1.

Due to oGP, CMC, Alg and $CaCl_2$, four factors have effect on microsphere preparation, and they can influence each other, so according to the results of single factor experiment, we design four factors and four levels orthogonal test to determine to the optimal preparing process of Guiqi polysaccharide/chitosan/sodium alginate composite hydrogel microspheres.

2.3 Microstructure Observation by SEM

To preserve their structure, hydrogel samples were rapidly frozen in viscous nitrogen, which obtained from liquid nitrogen placed under vacuum a few minutes to reach a temperature of -210°C. Then, they were deposited on a copper grid. After introducing the sample into the microscope chamber, the residual ice formed on its surface was completely eliminated by sublimation, heating the sample from -160°C to -80°C under reduced pressure. Hydrogels were cooled again at -160°C in order to fix the structure, then metal-coated with gold. They were observed on a Hitachi S800 microscope with a voltage between 5 and 10 kV. With this technique, the water contained in the hydrogels was neither removed nor crystallized thus preserving the gel microstructure.

2.4 Fourier Transform Infrared Spectroscopy Analysis

The absorption spectra of GPCH, GPAH and GPcM were obtained by FT-IR spectroscopy (Nicole Impact 410) in KBr pellet. The FT-IR spectra were recorded between 4000 cm^{-1} and 400 cm^{-1}.

2.5 Balanced Swelling Ratio (BSR)

Determine the equilibrium swelling ratio of the sample according to the method of Park [33]. Samples GPCH, GPAH, GPcM, GPcM-BSA were freeze-dried to constant weight, and M0 was weighed separately. Samples were placed in PBS buffer pH 7.4 and swollen at 37°C for 24 h. After the sample reached the swelling equilibrium, the sample was taken and the M24 was weighed. The formula for swelling *in vitro* is as follows:

$$BSR = \frac{M24 - M0}{M0} \times 100\% \quad (1)$$

2.6 Determination of Drug Loading Efficiency (LE) and Encapsulation Efficiency (EE) of GPcM

Weight 200 mg of dried drug-loaded GPcM, add 10 mL of 5% EDTA solution, ultrasonically to completely break the GPcM, take the supernatant after centrifugation, wash the precipitate twice by adding 5 mL of distilled water, then combine the supernatant, dilute to 2 mL with distilled water. Then, the protein content was measured at 280 nm. The encapsulation rate is calculated as:

$$EE = \frac{C1}{C} \times 100\% \quad (2)$$

$$LE = \frac{M1}{M} \times 100\% \quad (3)$$

C1: medicine content in microspheres. *C*: total drug content in microspheres and medium. *M1*: packaged drug mass. *M*: total microsphere mass.

2.7 Determination of Cumulative Release Rate of Composite Drug-loaded GPcM in vitro

The cumulative release rate of composite drug-loaded GPcM was detected in an Erlenmeyer flask containing 100 mL of phosphate buffer solution of PH = 7.4, shaking in a constant temperature water bath oscillator (37°C ± 5°C, rotation speed 50 rpm). 5 mL of release solution was taken out every 12 h and measured at 595 nm to calculate the drug concentration and the cumulative release amount. And the same amount of release medium was added after the release solution was removed.

2.8 Statistical Analysis

Analytical determinations were performed at least in triplicate. Values of different parameters were expressed as the mean ± standard deviation.

3 Results and Discussion

3.1 Analysis of GP, oGP and CMC

The content of polysaccharide in the extracted Guiqi polysaccharide was determined by the sulfuric a cid-phenol method, and the yield and polysaccharide content of the Guiqi polysaccharide were calculated. The yield of Guiqi polysaccharide was 6.3%. Further, the actual oxidation degree of the GP under $NaIO_4$ oxidation was 45.5%. The degree of substitution of CMC was 34.6%.

3.2 Evaluation of GPcM

The GPcM were successfully prepared using ES, and they are light yellow. As shown in Fig. 1, a common camera image of the microspheres shows that the GP polysaccharides chitosan alginate composite microspheres are spherical and have a smooth surface. Particle size is an important feature for microsphere application feasibility [34]. The smaller the particle size of the microspheres, the larger the specific surface area, the stronger the loading and encapsulation ability of the drug, and the more efficient drug loading during drug delivery. Thus, we selected minimum particle size as the optimization criterion to render the microspheres suitable for drug delivery.

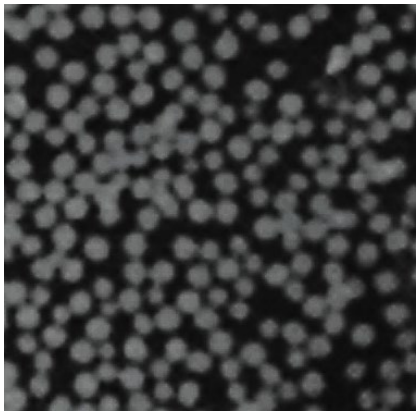

Figure 1: Morphology of GPcM

Fig. 2 shows the effect of voltage on the particle size of the GPcM in a single factor test. The particle size of the GPcM is different at different voltages. It can be seen from the figure that GPcM has the smallest particle size at 15 kV, so the particle size of GPcM is optimal at 15 kV. As shown in Tabs. 1 and 2, the optimum formulation has an average particle size of 420 μm. The results of the particle size distribution ranged from 395.1 μm to 841.5 μm. A1, B3, C2, and D2 are the optimal levels of A, B, C, and D, respectively. The optimal combination of the four factors is A1B3C2D2, that is, the optimal process conditions for preparing GPcM are 5% (*w*/*w*) GP, 1.5% (*w*/*w*) CS, 2% Alg (*w*/*w*) and $CaCl_2$ is 2% (*w*/*w*).

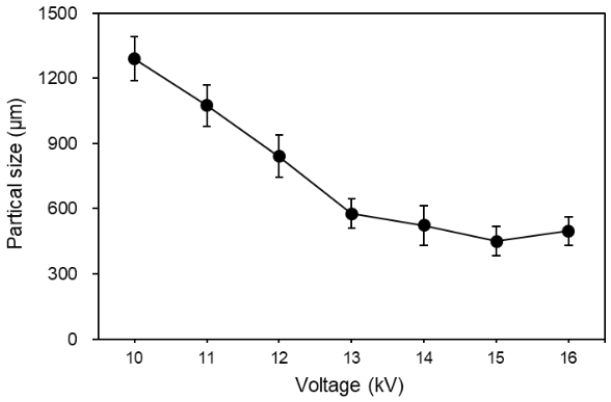

Figure 2: Effect of voltage on particle size of microspheres

Table 1: Optimal particle size screening test factor level table

Factors Levels	oGP (w/v) A	CMC (w/v) B	Alg (w/v) C	$CaCl_2$(w/v) D
1	0.5	0.5	1.0	1.0
2	1.0	1.0	2.0	2.0
3	1.5	1.5	3.0	3.0
4	2.0	2.0	4.0	4.0

Table 2: The $L_{16}(4^4)$ orthogonal design and experimental results

Number	Factors				The average particle size (μm)
	A	B	C	D	
1	0.5	1.0	2.0	2.0	879.1
2	1.0	2.0	1.0	2.0	761.4
3	1.5	2.0	2.0	2.0	1043.9
4	2.0	1.0	1.0	1.0	1635.8
5	0.5	1.5	1.0	2.0	399.3
6	1.0	0.5	2.0	1.0	531.5
7	1.5	0.5	1.0	2.0	572.6
8	2.0	1.5	2.0	2.0	781.0
9	0.5	0.5	4.0	2.0	528.9
10	1.0	1.5	2.0	2.0	420.4
11	1.5	1.5	2.0	1.0	421.4
12	2.0	0.5	2.0	2.0	705.5
13	0.5	2.0	2.0	1.0	395.1
14	1.0	1.0	2.0	2.0	841.5

15	1.5	1.0	2.0	2.0	396.4
16	2.0	2.0	2.0	2.0	603.3
K1	2202.4	2338.5	3369.1	2983.8	
K2	2554.8	3752.8	1917.4	2467.7	
K3	2434.3	2022.1	3235.5	2475.4	
K4	3725.6	2506.7	2449.1	2990.2	
k1	550.6	584.6	842.3	745.9	
k2	638.7	938.2	479.4	616.9	
k3	608.6	505.5	808.9	618.8	
k4	931.4	626.7	612.3	747.6	
Range (R)	380.3	432.7	362.9	130.7	
order	B > A > C > D				
Excellent level	A1	B3	C2	D2	
Excellent combination	A1B3C2D2				

3.3 FT-IR Spectrum of GQPH, ASH and GPcM

FT-IR spectroscopy of samples in a range of 4000-400 cm^{-1} is shown in Fig. 3. In the Fig. 3(A), the strong absorption peak between 3600 and 3200 cm^{-1}corresponded to the stretching vibration of hydroxyl group and amino group [35]. The weak band recorded at 2920 cm^{-1} was related to C-H stretching vibration including -CH, $-CH_2$ and $-CH_3$. The peak obtained at 2366 cm^{-1} was from the aliphatic C-H bonds [36]. The relatively strong absorption peak recorded at 1735 cm^{-1} indicated the presence of carbonyl group [37]. In the FT-IR diagram of oGP, there was an absorption peak at 1735 cm^{-1}. The absorption at 1735 cm^{-1} in the hydrogel GPCH was weakened. It indicated that oGP and CMC were chemically crosslinked, and therefore, the carbonyl content was reduced. The large band obtained at 1080 cm^{-1} corresponded to stretching vibration of C-O in O=C-H bonds and C=O=C glyosidic bond vibration and it was related to the presence of pyranose ring in polysaccharides [38]. In the infrared image of GPAH, the strong absorption peak between 3600 cm^{-1} and 3200 cm^{-1} corresponded to the stretching vibration of hydroxyl group and carboxyl group. 2970 cm^{-1} was related to stretching vibration of O-H. The peak at 1600-1900 cm^{-1} indicated the presence of carbonyl group. Some peaks recorded at 1000-1250 cm^{-1} indicated that there was a C-O single bond. In Fig. 3(B), various functional groups of GPCH and GPAH are shown compared to the infrared images of GPCH, GPAH and GPcM, indicating that the two crosslinks are independent and hybrid to form an interpenetrating network system. This ensures that the biological properties of each material are not destroyed and at the same time demonstrates the structure of the interpenetrating network system.

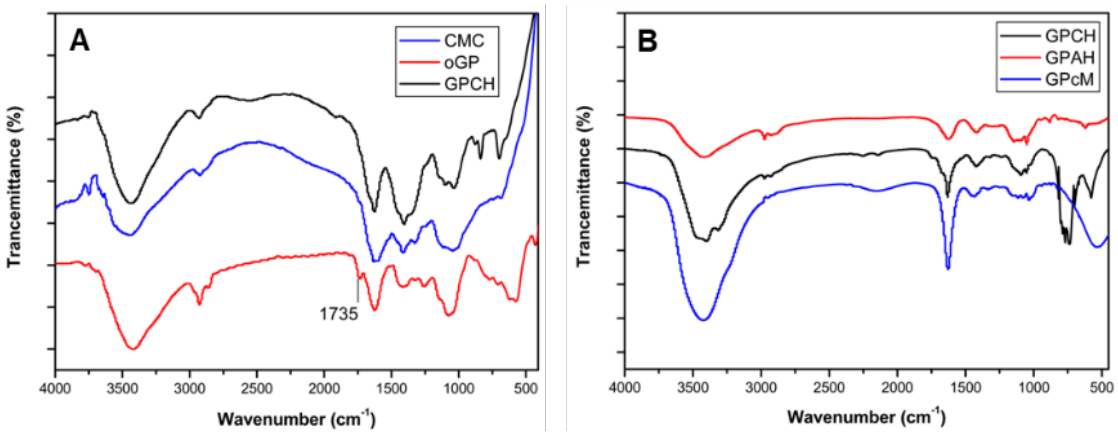

Figure 3: FT-IR spectrum of GPCH (A), comparison of different hydrogel samples (B)

3.4 Micro-Structure of the GPcM

As can be seen from Fig. 4, the compound GPcM samples had porous structure. GP and CS were chemically cross-linked into a pore-like structure, and cross-linking of Alg and $CaCl_2$ gave a network structure. GPcM has a small pore size and a uniform small void. The reason may be that the two cross-linking systems coexisting lead to an increase in cross-linking density and strength. The morphology of the hydrogel microspheres affects the release rate of the drug to some extent, so the presence of these two crosslinks may affect some properties of the microspheres.

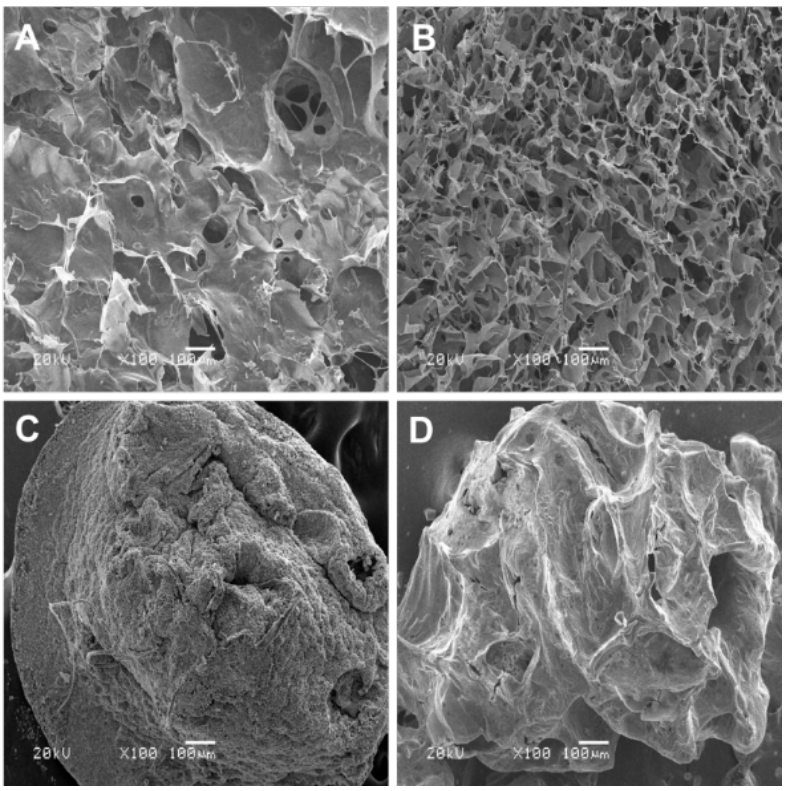

Figure 4: SEM images of the samples. (A) GPCH, (B) GPAH, (C) GPcM, (D) GPcM-BSA

3.5 Balanced Swelling Ratio (BSR)

Fig. 5 shows the *in vitro* equilibrium swelling ratio of different samples. The swelling ability of both GPCH and GPAH hydrogels were significantly inferior to that of hydrogel microspheres. The swelling capacity of GPcM and GPcM-BSA were similar, reaching 1300%. It showed that GPcM had good water retention capacity.

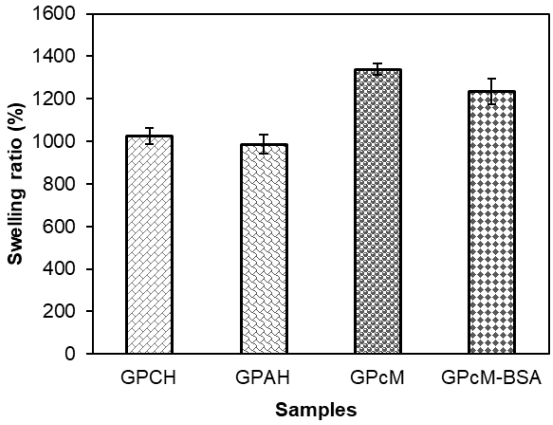

Figure 5: Balanced swelling ratio (BSR) of GPCH, GPAH, GPcM, and GPcM-BSA

3.6 Determination of Drug Loading (LE) and Encapsulation Efficiency (EE) of GPcM

Encapsulation efficiency, drug loading content and particle size are key physicochemical properties of microspheres. Encapsulation efficiency and drug loading content are important in assessing the drug loading capacity of microspheres [39]. Therefore, maximum entrapment efficiency and drug loading content were chosen as the two responses of preparation condition optimization. The experiment showed that the drug LE and EE of the GPcM were 56.3% ± 5.4% and 72.6% ± 4.9%.

3.7 In vitro Release Study

The cumulative release profile of BSA from composite GPcM (pH 7.4) in PBS is depicted in Fig. 6. The curve shows that the release behavior consisted of two phases. The first stage was burst release, which can be attributed to the adsorption of BSA on the surface of the GPcM or in the surface layer. Over time, the embedded drug readily diffusec from the polymer matrix during the initial incubation time (0-24 h). The second phase of release is relatively stable because the mechanism of drug release converted into diffusion release and dissolution release. In this period (24-144 h), the release of the BSA was accompanied by the degradation of the GPcM.

Compared with the stable release of GPcM in 72 h, the GPcM would first reach the theoretical blood concentration by burst release, and then stably released till 144 h. Moreover, the GPCH was severely broken after 96 h, that is, degradation occurred. At the same time, the GPcM were intact and the drug was released stably.

The cumulative release profile of BSA in PBS from BSA-loaded complex GPcM pH 7.4 and 1.2 is depicted in Fig. 7. This curve showed similar release of BSA during simulated intestinal fluid and simulated gastric fluid release behavior. In the early stage, the drug reached the blood concentration by burst release, and later reached a slow release effect. The acid stability of GPcM was also indirectly demonstrated by comparison of different pH values.

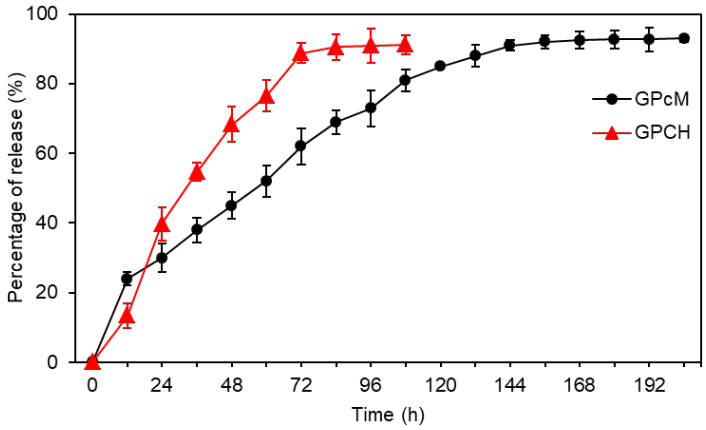

Figure 6: Comparison of BSA release of GPcM and GPCH

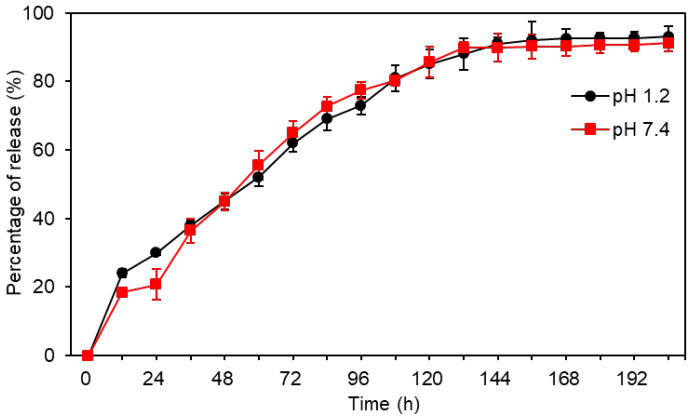

Figure 7: Comparison of BSA release in microspheres at different pH

4 Conclusion

Compared with that of CS hydrogels, interpenetrating network in GPcM hydrogel microspheres can prolong the release of BSA *in vitro*. In addition, GPcM ensures that the biological properties of various polymeric materials are unaffected and also promotes an increase in crosslink density. *In vitro* studies have shown that GPcM has the potential of encapsulate, loading macromolecular drugs, and delivering small molecule drugs. Further research on its performance with animal models is currently underway. Together, it will promote our understanding of interpenetrating network systems and provide advanced strategies for the clinical application of hydrogel microspheres.

Acknowledgement: This work was supported in part by National Natural Science Foundation of China (81560737, 31860250), Natural Science Foundation of Gansu Province (18JR3RA148), Guangxi Provincial Natural Science Fund of China (2016GXNSFAA380234), and Fundamental Research Funds for Key Laboratory of Drug Screening and Deep Processing for Traditional Chinese and Tibetan Medicine of Gansu Province (20180801).

References

1. Shi, X. D., Sun, P. J., Gan, Z. H. (2018). Preparation of porous polylactide microspheres and their application in tissue engineering. *Polymer Science, 36(6),* 712-719.

2. Fattl, E., Roques, B., Puisieux, F., Blancoprieto, M. J., Couvreur, P. (1997). Multiple emulsion technology for the design of microspheres containing peptides and oligopeptides. *Advanced Drug Delivery Reviews, 28(1),* 85-96.
3. Kavas, A., Keskin, D., Altunbas, K., Tezcaner, A. (2016). Raloxifene-/raloxifene-poly (ethylene glycol) conjugate-loaded microspheres: a novel strategy for drug delivery to bone forming cells. *Pharmaceutics, 510(1),* 168-183.
4. Zhang, J., Chen, X. G., Liu, C. S. (2009). Investigation of polymeric amphiphilic nanoparticles as antitumor drug carriers. *Materials Science-Materials in Medicine, 20(4),* 991-999.
5. Rokhade, A. P., Kulkarni, P. V., Mallikarjuna, N. N., Aminabhavi, T. M. (2009). Preparation and characterization of novel semi-interpenetrating polymer network hydrogel microspheres of chitosan and hydroxypropyl cellulose for controlled release of chlorothiazide. *Microencapsulation, 26(1),* 27-36.
6. Ganguly, K., Aminabhavi, T. M., Kulkarni, A. R. (2011). Colon targeting of 5-fluorouracil using polyethylene glycol cross-linked chitosan microspheres enteric coated with cellulose acetate phthalate. *Industrial & Engineering Chemistry Research, 50(21),* 11797-11807.
7. Fang, Y. Y., Wang, L. J., Li, D., Li, B. Z., Bhandari, B. et al. (2008). Preparation of crosslinked starch microspheres and their drug loading and releasing properties. *Carbohydrate Polymers, 74(3),* 379-384.
8. Kurkuri, M. D., Kulkarni, A. R., Kariduraganavar, M. Y., Aminabhavi, T. M. (2001). *In vitro* release study of verapamil hydrochloride through sodium alginate interpenetrating monolithic membranes. *Drug Development and Industrial Pharmacy, 27(10),* 1107-1116.
9. Zhang, X. L., Hui, Z. Y., Wan, D. X., Huang, H. T., Huang, J. et al. (2010). Alginate microsphere filled with carbon nanotube as drug carrier. *Biological Macromolecules, 47(3),* 389-395.
10. Zhang, Z. F., Jin, J., Shi, L. G. (2008). Antioxidant activity of the derivatives of polysaccharide extracted from a Chinese medical herb (Ramulusmori). *Food Science and Technology Research, 14(2),* 160-168.
11. Li, X. T., Zhang, Y. K., Kuang, H. X., Jin, F. X., Liu, D. W. et al. (2012). Mitochondrial protection and anti-aging activity of Astragalus polysaccharides and their potential mechanism. *Molecular Sciences, 13(2),* 1747-1761.
12. Kuang, X., Yao, Y., Du, J. R., Liu, Y. X., Wang, C. Y. et al. (2006). Neuroprotective role of Z-ligustilide against forebrain ischemic injury in ICR mice. *Brain Research, 1102(1),* 145-153.
13. Wu, S. J., Ng, L. T., Lin, C. C. (2004). Antioxidant activities of some common ingredients of traditional Chinese medicine, Angelica sinensis, Lycium barbarum and Poriacocos. *Phytotherapy Research, 18(12),* 1008-1012.
14. Han, S. B., Kim, Y. H., Lee, C. W., Park, S. M., Lee, H. Y. et al. (1998). Characteristic immunostimulation by angelan isolated from Angelica gigas Nakai. *Immunopharmacology, 40(1),* 39-48.
15. Pu, X. Y., Wang, H. R., Li, Y., Fan, W. B., Yu, S. (2013). Antiviral activity of Guiqi polysaccharides against enterovirus 71 *in vitro*. *Virologica Sinica, 28(6),* 352-359.
16. Zhou, W. J., Wang, S., Hu, Z., Zhou, Z. Y., Song, C. J. (2015). Angelica sinensis polysaccharides promotes apoptosis in human breast cancer cells via CREB-regulated caspase-3 activation. *Biochemical & Biophysical Research Communications, 467(3),* 562-569.
17. Pu, X. Y., Yu, S., Fan, W., Liu, L., Ma, X. L. et al. (2015). Guiqi polysaccharide protects the normal human fetal lung fibroblast WI-38 cells from H2O2-induced premature senescence. *Clinical and Experimental Pathology, 8(5),* 4398-4407.
18. Yang, B., Xiao, B., Sun, T. (2013). Antitumor and immunomodulatory activity of Astragalus membranaceus polysaccharides in H22 tumor-bearing mice. *Biological Macromolecules, 62(11),* 287-290.
19. Croisier, F., Jérôme, C. (2013). Chitosan-based biomaterials for tissue engineering. *European Polymer Journal, 49(4),* 780-792.
20. Pourjavadi, A., Kurdtabar, M., Mahdavinia, G. R., Hosseinzadeh, H. (2006). Synthesis and super-swelling behavior of a novel protein-based superabsorbent hydrogel. *Polymer Bulletin, 57(6),* 813-824.
21. Dubnika, A. D., Loca, L., Berzina, C. (2012). Functionalized hydroxyapatite scaffolds coated with sodium alginate and chitosan for controlled drug delivery. *Proceedings of the Estonian Academy of Sciences, 61(3),* 193-199.
22. Khan, M. K. I., Mujawar, L. H., Schutyser, M. A. I., Karin, S., Remko, B. (2013). Deposition of thin lipid films prepared by electrospraying. *Food & Bioprocess Technology, 6(11),* 3047-3055.

23. Barringer, S. A., Sumonsiri, N. (2015). Electrostatic coating technologies for food processing. *Annual Review of Food Science & Technology, 6(1),* 157-169.
24. Zhong, Y., Cavender, G., Zhao, Y. Y. (2014). Investigation of different coating application methods on the performance of edible coatings on Mozzarella cheese. *LWT-Food Science and Technology, 56(1),* 1-8.
25. Kessick, R., Fenn, J., Tepper, G. (2004). The use of AC potentials in electrospraying and electrospinning processes. *Polymer, 45(9),* 2981-2984.
26. Wu, Y. (2009). Study on procedure optimization of the extraction of polysaccharides and regularities of distribution in Angelica sinensis. *Food Science & Technology, 34(2),* 216-219.
27. Wang, S. C., Shan, J. J., Wang, Z. T., Hu, Z. B. (2006). Isolation and structural analysis of an acidic polysaccharide from Astragalus membranaceus (Fisch.) Bunge. *Integrative Plant Biology, 48(11),* 1379-1384.
28. Zhang, W. J., Wang, X. C., Ma, J. Z., Zhao, L., Yang, C. G. et al. (2017). Preparation of chitosan/pumpkin polysaccharide hydrogel for potential application in drug delivery and tissue engineering. *Porous Materials, 24(2),* 497-506.
29. Zhao, H., Heindel, N. D. (1991). Determination of degree of substitution of formyl groups in polyaldehyde dextran by the hydroxylamine hydrochloride method. *Pharmaceutical Research, 8(3),* 400-402.
30. Chen, X. G., Park, H. J. (2003). Chemical characteristics of O-carboxymethyl chitosans related to the preparation conditions. *Carbohydrate Polymers, 53(4),* 355-359.
31. Mourya, V. K., Inamdar, N. N., Choudhari, Y. M. (2011). Chitooligosaccharides: synthesis, characterization and applications. *Polymer Science Series A, 53(7),* 583-612.
32. He, P., Davis, S. S., Illum, L. (1999). Chitosan microspheres prepared by spray drying. *International Journal of Pharmaceutics, 187(1),* 53-65.
33. Park, H., Guo, X., Temenoff, J. S., Tabata, Y., Caplan, A. I. et al. (2009). Effect of swelling ratio of injectable hydrogel composites on chondrogenic differentiation of encapsulated rabbit marrow mesenchymal stem cells *in vitro*. *Biomacromolecules, 10(3),* 541-546.
34. Agnihotri, S. A., Mallikarjuna, N. N., Aminabhavi, T. M. (2004). Recent advances on chitosan-based microand nanoparticles in drug delivery. *Journal of Controlled Release, 100(1),* 5-28.
35. Mao, S. R., Guo, C. Q., Shi, Y., Li, L. C. (2012). Recent advances in polymeric microspheres for parenteral drug delivery-part 1. *Expert Opinion on Drug Delivery, 9(9),* 1161-1176.
36. Ballesteros, L. F., Cerqueira, M. A., Teixeira, J. A., Mussatto, S. I. (2015). Characterization of polysaccharides extracted from spent coffee grounds by alkali pretreatment. *Carbohydrate Polymers, 127(3),* 347-354.
37. Ghribi, A. M., Sila, A., Gafsi, I. M., Blecker, C., Danthine, S. et al. (2015). Structural, functional, and ACE inhibitory properties of water-soluble polysaccharides from chickpea flours. *International Journal of Biological Macromolecules, 75(4),* 276-282.
38. Zhang, L., Tu, Z. C., Wang, H., Kou, Y., Wen, Q. H. et al. (2015). Response surface optimization and physicochemical properties of polysaccharides from Nelumbonucifera leaves. *International Journal of Biological Macromolecules, 74(3),* 103-110.
39. Shahzad, M. K., Ubaid, M., Murtaza, G. (2012). Formulation and optimization of celecoxib-loaded microspheres using response surface methodology. *Tropical Journal of Pharmaceutical Research, 11(5),* 695-702.